Developmental Cell
Article

Lgl1 Activation of Rab10 Promotes Axonal Membrane Trafficking Underlying Neuronal Polarization

Tong Wang,[1,2] Yang Liu,[1,2] Xiao-Hui Xu,[1] Cai-Yun Deng,[1] Kong-Yan Wu,[1] Ji Zhu,[1] Xiu-Qing Fu,[1] Miao He,[1] and Zhen-Ge Luo[1,*]

[1]Institute of Neuroscience and State Key Laboratory of Neuroscience, Shanghai Institutes for Biological Sciences, Chinese Academy of Sciences, 320 Yue Yang Road, Shanghai 200031, China

[2]These authors contributed equally to this work

*Correspondence: zgluo@ion.ac.cn

DOI 10.1016/j.devcel.2011.07.007

SUMMARY

Directed membrane trafficking is believed to be crucial for axon development during neuronal morphogenesis. However, the underlying mechanisms are poorly understood. Here, we report a role of Lgl1, the mammalian homolog of *Drosophila* tumor suppressor Lethal giant larvae, in controlling membrane trafficking underlying axonal growth. We find that Lgl1 is associated with plasmalemmal precursor vesicles and enriched in developing axons. Lgl1 upregulation promoted axonal growth, whereas downregulation attenuated it as well as directional membrane insertion. Interestingly, Lgl1 interacted with and activated Rab10, a small GTPase that mediates membrane protein trafficking, by releasing GDP dissociation inhibitor (GDI) from Rab10. Furthermore, Rab10 lies downstream of Lgl1 in axon development and directional membrane insertion. Finally, both Lgl1 and Rab10 are required for neocortical neuronal polarization in vivo. Thus, the Lgl1 regulation of Rab10 stimulates the trafficking of membrane precursor vesicles, whose fusion with the plasmalemma is crucial for axonal growth.

INTRODUCTION

The Lethal (2) giant larvae (Lgl) protein of *Drosophila*, initially characterized as a tumor suppressor (Bilder et al., 2000; Gateff, 1978), regulates a variety of polarization processes, including epithelial polarity formation, asymmetric cell division, and directed cell migration (Hutterer et al., 2004; Ohshiro et al., 2000; Peng et al., 2000). During these processes, Lgl was found to be crucial for targeting specific proteins to subcellular domains (Wirtz-Peitz and Knoblich, 2006), but the mechanism by which Lgl regulates these processes is poorly understood. The mammalian homolog Lgl1 is enriched in the brain (Klezovitch et al., 2004), and *Lgl1* gene deletion in mice caused the loss of asymmetric cell division of neural progenitor cells, leading to defects in cell cycle exit and tumorigenesis in the brain (Klezovitch et al., 2004). Interestingly, Lgl1 is regulated by atypical protein kinase C (aPKC) (Betschinger et al., 2003; Plant et al., 2003) and Disheveled (Dvl) (Dollar et al., 2005), both of which are known to regulate neuronal polarity (Shi et al., 2003; Zhang et al., 2007).

The process of neuronal polarization begins with the initiation of a fast-growing axon that demands a large amount of new membrane addition from the intracellular supply (Pfenninger, 2009; Ye et al., 2006). The molecular mechanisms controlling this process remain largely unknown. Different members of Rab family small GTPases play important roles in various membrane trafficking events, including formation of transport vesicles and their translocation, docking and fusion in eukaryotic cells (Grosshans et al., 2006; Stenmark, 2009). Among more than 60 mammalian Rabs, Rab10 is shown recently to mediate trafficking of membrane proteins to the plasmalemma in non-neuronal cells (Sano et al., 2007). Like other small GTPases, Rab proteins can be activated by guanine exchange factors (GEFs), which trigger the exchange of GDP by GTP, and inactivated by GTPase-activating proteins (GAPs) via hydrolysis of the bound GTP to GDP (Pfeffer, 2001). In addition, Rab proteins undergo the cycle of GDP dissociation inhibitor (GDI) association and dissociation, as well as membrane detachment and attachment, with the GDI dissociation and membrane attachment stimulating Rab activation (Grosshans et al., 2006; Pfeffer, 2005; Seabra and Wasmeier, 2004). Both the function and regulation of Rab proteins in the membrane trafficking underlying neuronal morphogenesis are poorly understood.

In this work, we have identified Lgl1 as an activator for Rab10 and demonstrated that Lgl1 regulates membrane trafficking and axon development via its action on Rab10.

RESULTS

Expression of Lgl1 in the Developing Brain and Cultured Neurons

The specificity of anti-Lgl1 antibody was determined by western blot analysis of cultured cortical neurons transfected with Myc-Lgl1 or small interference RNA (siRNA) against Lgl1 ("siLgl") (see Figure S1A available online). Western blots of whole-brain extracts showed that Lgl1 is highly expressed in the embryonic and postnatal rat brain (Figure S1B). In agreement with the finding that Lgl1 regulates asymmetric division of neural progenitor cells (Klezovitch et al., 2004), we found that Lgl1 was highly expressed in ventricular (VZ) and subventricular (SVZ) zones (Figure S1C). Furthermore, Lgl1 was also expressed in postmitotic β-tubulin III (Tuj1) positive neurons in the cortical plate

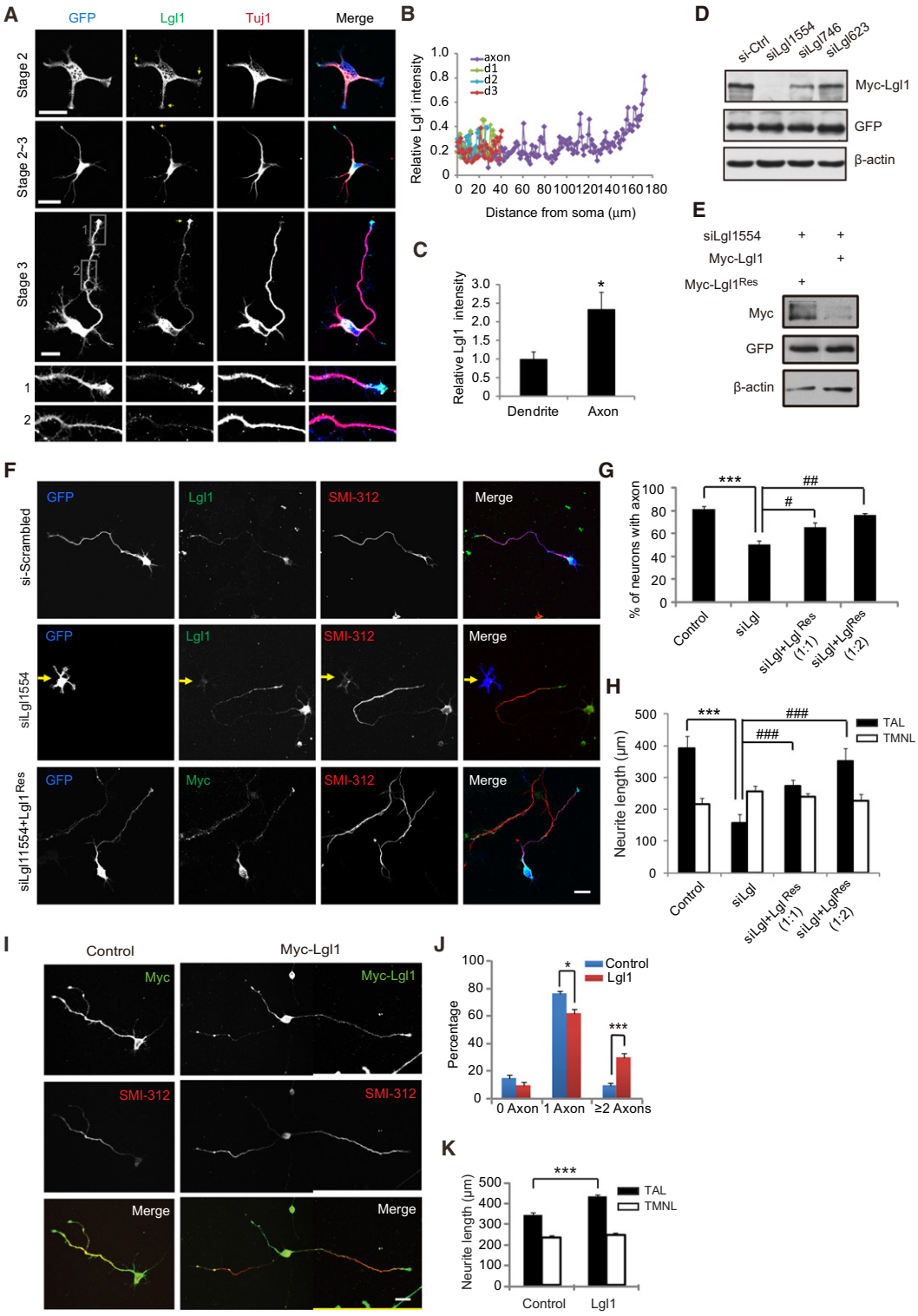

Figure 1. Lgl1 Is Required for Axon Development in Cultured Hippocampal Neurons

(A) GFP-transfected hippocampal neurons at different stages (1–3 DIV) were stained for Lgl1 and Tuj1. Arrows indicate neurite or axonal growth cones. Boxed areas (1 and 2) show axonal growth cone and shaft, respectively. Scale bar, 20 μm.

(B) Relative immunofluorescence intensity of Lgl1 over GFP in the processes of a stage 3 neuron was plotted against the distance from soma.

(C) Relative immunofluorescence intensity of Lgl1 at axonal or dendritic neurites. The ratio of the intensity of Lgl1 against that of GFP in dendrites was taken as 1.0. The values were obtained from six neurons. *$p < 0.05$, Student's t test.

(D) Knockdown effects of siRNAs on ectopic-expressed Myc-Lgl1 in HEK293 cells. Cotransfected GFP was used as control.

(CP) (Figure S1C) and the adult hippocampal neurons (Figure S1D). Next, we determined subcellular distribution of Lgl1 and found that Lgl1 was mainly distributed in crude membrane fractions of the P0 rat cortex (Figure S1E). Further fractionation of the extract for membrane vesicles using OptiPrep density gradient showed that Lgl1 is distributed to distinct fractions that partially overlapped with those for early endosome marker EEA1, trans-Golgi network marker TGN38, or *cis*-Golgi marker GM130 (Figures S1F and S1G). Thus, Lgl1 is localized to membrane compartments in the brain.

We next determined subcellular localization of Lgl1 in isolated neurons using immunostaining. Isolated hippocampal neurons from rat embryos undergo spontaneous polarization in culture (Dotti et al., 1988; Goslin and Banker, 1989). Shortly after adherence to the culture substratum, these neurons extend several short neurites (stage 2). After 24 hr, however, one of the neurites exhibits accelerated growth and becomes the axon (stage 3). To determine subcellular localization of Lgl1 during axon specification, dissociated hippocampal neurons were transfected with GFP to mark neurite volume, and then stained with antibodies against Lgl1 and Tuj1 at different stages. In stage 2 neurons (1 day in vitro [DIV]), Lgl1 was present in vesicular-like structures in the soma and the growth cone, as well as shaft, of all neurites (Figure 1A). However, in neurons during the transition from stage 2 to stage 3, Lgl1 appeared to be enriched in the tip of the longest neurite (Figure 1A, the second row from top, indicated by arrows). By stage 3, vesicular Lgl1 was abundant in axonal shafts and in growth cones but was largely absent from dendrites (Figure 1A). The identity of the longest neurite as an axon was determined by staining with axonal marker SMI-312 (Figure 1F). Using transfected GFP as marker for the neurite volume, we found that Lgl1 staining was indeed significantly higher in the axon than in the dendrite of stage 3 neurons (Figures 1B and 1C). These results suggest a correlation between polarized Lgl1 localization and neurite outgrowth and thus prompted us to investigate the role of Lgl1 in axon development.

Lgl1 Is Required for Axon Development in Cultured Hippocampal Neurons

A siRNA (siLgl1554) against rat Lgl1 was prepared, and its effectiveness in suppressing Lgl1 expression was shown in cultured HEK293 cells (Figure 1D) and primary neurons (Figure 1F). Transfection of cultured hippocampal neurons before cell plating with a plasmid encoding siLgl resulted in reduced immunostaining of endogenous Lgl1 (Figure 1F, see the cell indicated by arrows in the middle row), and a marked reduction in axon formation and axon growth (Figures 1F–1H), as compared to cultures transfected with control (scrambled) siRNA. The reduction of axon formation was reflected by the reduced percentage of neurons with axons, which were positively stained with SMI-312 (Figures 1F and 1G). In addition, we measured the total length of axons (TAL), including branches, in each cell and found that it was significantly shorter in neurons with Lgl1 knockdown ($p < 0.001$, siLgl versus scrambled siRNA) (Figure 1H). Of note, Lgl1 downregulation had no effect on total length of minor neurites (TMNL) (Figure 1H), suggesting the specific role of Lgl1 in axon growth. The effect of siLgl on axon development could be significantly prevented by coexpressing $Lgl1^{Res}$, the siRNA-resistant form of Lgl1 (Figures 1E–1H), thus excluding potential off-target effects of siRNA.

Next, we determined the gain-of-function effect of Lgl1 by overexpressing Myc-Lgl1 in cultured hippocampal neurons. We found that overexpression of Lgl1 increased the axon growth, as shown by the increased percentage of neurons with multiple axons ($\geq$2 axons) (Figures 1I and 1J) and the TAL, but had no effect on TMNL (Figure 1K). Thus, Lgl1 plays an important role in axon development.

Lgl1 Acts Upstream of Rab10 in Promoting Axon Development

Next, we investigated the mechanisms by which Lgl1 affects axon development. In *S. cerevisiae*, the Lgl orthologs Sro7p and Sro77p regulate polarized exocytosis (Lehman et al., 1999; Zhang et al., 2005), probably by interacting with the exocyst complex (Zhang et al., 2005) or Sec4p (Grosshans et al., 2006), one of the 11 yeast Rabs involved in membrane trafficking. Out of more than 60 mammalian Rabs, we screened 6 that have high homology with yeast Sec4p and found that Lgl1 interacts strongly with Rab10 when coexpressed in HEK293 cells, as shown by coimmunoprecipitation (co-IP) of Myc-Lgl1 with hemagglutinin (HA)-tagged Rab10, but not with Rab5a, 8b, 11, or 13, and weakly with Rab8a (Figure 2A). Furthermore, Lgl1 coprecipitated with native endogenous Rab10 extracted from membrane fractions of cultured cortical neurons (Figures 2B and 2C), suggesting that the Lgl1/Rab10 interaction also exists in vivo.

Given the role of Rab10 in membrane protein trafficking in nonneuronal cells (Sano et al., 2007) and its interaction with Lgl1, we sought to determine the role of Rab10 in axon development. First, we determined the distribution of Rab10 in cultured hippocampal neurons transfected with GFP as marker for the neurite volume (Figure S2A). We found that, similar to Lgl1, Rab10 exhibited vesicular distribution in the soma and growth cones of all neurites of stage 2 neurons (Figure S2A, the top row). During the transition from stage 2 to 3, Rab10 was enriched in the growth cone of the longest neurite (Figure S2A, the second row). By stage 3, Rab10 was largely distributed in the distal part of axons, rather than dendrites (Figures S2A, the third row,

(E) HEK293 cells were cotransfected with pSUPER-siLgl1554 and Myc-Lgl1 or siRNA-resistant Lgl1 (Myc-$Lgl1^{Res}$). Resulting cell lysates were subject to IB with indicated antibodies.

(F–H) Rat hippocampal neurons were transfected with pSUPER-siLgl that encodes siRNA1554 or scrambled siRNA or siLgl plus different amount of Myc-$Lgl1^{Res}$ (siLgl1/$Lgl1^{Res}$, 1:1 or 1:2), and then stained with SMI-312 and Lgl1 or Myc antibodies at 3 DIV. Cotransfected GFP is used to mark transfected neurons. Arrows indicate the neuron transfected with siLgl.

(G) Quantitative analysis for percentage of neurons with at least one axon.

(H) Quantitative analysis for TAL and TMNL.

(I) Hippocampal neurons transfected with GFP, either alone or together with Myc-Lgl1, were stained with SMI-312 antibody at 3 DIV.

(J and K) Quantitative analysis for neuronal polarity (J) and neurite length (K). Data are shown as mean ± SEM. At least 54 neurons from three independent experiments were analyzed. *$p < 0.05$, **$p < 0.01$, ***$p < 0.001$. ANOVA with Student's t test. Scale bar represents 50 μm. See also Figure S1.

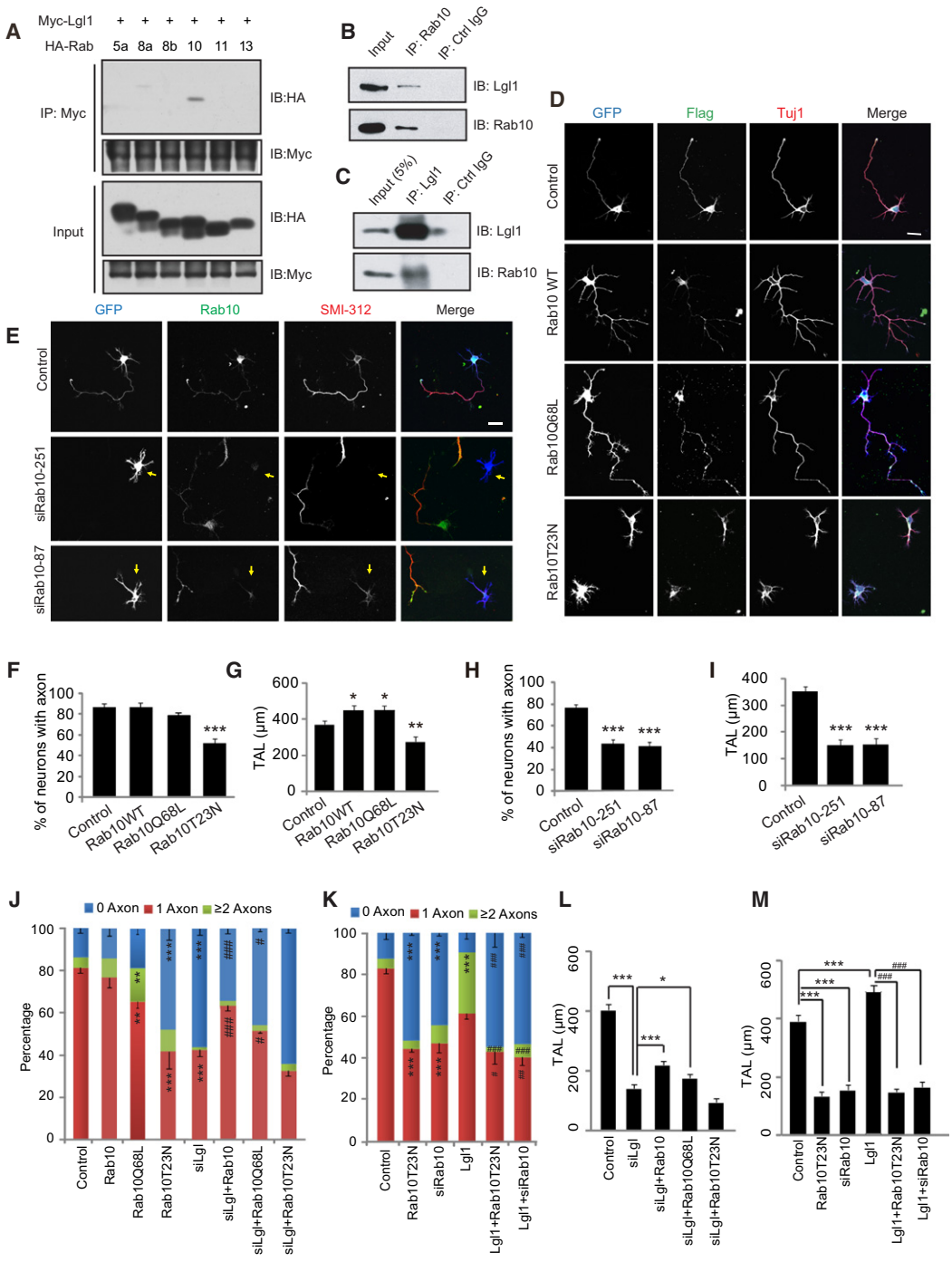

Figure 2. Rab10 Acts Downstream of Lgl1 for Axon Development

(A) Cell lysates from HEK293 cells transfected with indicated plasmids were subject to IP, and then IB with indicated antibodies.

(B and C) Crude membrane fractions (500 μg) of cortical neurons were subject to IP with mouse anti-Rab10 (B) or rabbit anti-Lgl1 (C), or normal control IgG, conjugated to either CNBr Sepharose (B) or protein A agarose (C) beads.

(D) Rat hippocampal neurons were transfected with GFP vector or together with Flag-tagged Rab10 constructs, and then stained with indicated antibodies at 3 DIV.

(E) Hippocampal neurons were transfected with pSUPER vector encoding siRNAs against Rab10 (siRNA251 or 87) or scrambled sequence (control). Arrows indicate cells transfected with siRab10.

(F–I) Quantification for the percentage of neurons with at least one axon (F and H) and TAL (G and I).

(J–M) Quantification for neuronal polarity (J and K) and TAL (L and M) of neurons transfected with various plasmid combinations. Results are shown as mean ± SEM of three independent experiments with a total of at least 90 neurons. *$p < 0.05$, **$p < 0.01$, ***$p < 0.001$ (compared to control); #$p < 0.05$, ##$p < 0.01$, ###$p < 0.001$ (compared to siLgl in J or Lgl1 in K and M); ANOVA with Student's t test. Scale bars represent 50 μm. See also Figure S2.

and S2B). Quantitatively, the relative intensity of Rab10 in axons was around 2-fold of that in dendrites (Figure S2C). Indeed, Lgl1 was partially colocalized with Rab10 in differentiating axons (Figure S2D), but to a lesser extent with GM130 or EEA1 (Figures S2E and S2F). Interestingly, downregulation of Lgl1 led to diffuse distribution of Rab10 (Figure S2G), and upregulation of Lgl1 caused enrichment of Rab10 in the tips and shafts of multiple axons (Figure S2H). Thus, Rab10 localization is associated with axon specification and regulated by Lgl1.

Having determined the interaction between Lgl1 and Rab10 and polarized distribution of Rab10, we next explored the role of Rab10 in neuronal polarization by transfecting hippocampal neurons with a wild-type (WT) or mutated forms of Rab10. We found that about half of neurons transfected with dominant-negative form of Rab10 (Rab10 ^{T23N}) remained at stage 2, with only short neurites and without detectable axon at 3 DIV (Figures 2D and 2F). We also compared axonal growth and found that neurons transfected with WT or constitutive-active form (Q68L) of Rab10 usually exhibited an axon with many branches and enhanced TAL (Figures 2D and 2G), compared to control cells transfected with GFP alone. In contrast, transfection with Rab10 ^{T23N} reduced axonal growth (Figures 2D and 2G). These results suggest that Rab10 activation promotes axonal growth. Given that different Rabs may share common regulators or effectors, the role of Rab10 in the participation of axon development was further determined by downregulating the expression of Rab10. We found that downregulating Rab10 by transfection of two effective siRNAs (Sano et al., 2007) (Figure S2I and Figure 2E) markedly reduced the percentage of neurons with axon (Figures 2E and 2H), and decreased axonal length (Figure 2I), whereas transfection of the corresponding scrambled siRNA controls had no effect. Similar to the effect of siLgl, siRNA of Rab10 (siRab10) had no effect on the TMNL (Figure S2L). These effects of siRab10 on axon development could be prevented by overexpressing the siRNA-resistant Rab10^{Res} (Figures S2J–S2L). We also determined the role of Rab8a and 13, which are closely related to Rab10, in neuronal polarization. We found that downregulating Rab8a by transfection of effective siRNA (Ishikura and Klip, 2008) markedly inhibited axon development (Figures S2M–S2O), whereas siRNA for Rab13 (Sun et al., 2010) had no effect (Figures S2M–S2O), in agreement with the previous observation that Rab8 controls neuronal morphogenesis (Huber et al., 1995). Together, these results indicate that Rab10 is a positive regulator for axon development.

The aforementioned gain- or loss-of-function approaches were also used to determine the relation between Lgl1 and Rab10 in regulating axon development. We found that overexpression of the WT or Q68L, but not T23N, form of Rab10 partially rescued the axon development defects in cells with depletion of endogenous Lgl1, as shown by the percentages of 1 Axon and 0 Axon populations and the TAL (Figures 2J and 2L). In addition, transfection with Rab10^{T23N} or siRab10 prevented the axon growth-promoting effect of Lgl1, whereas overexpressing Lgl1 had no effect on axonal defects caused by either Rab10^{T23N} or siRab10 (Figures 2K and 2M). Although downregulation of Rab8a or overexpression of dominant-negative form of Rab8 (T22N) prevented neuronal polarization (Figures S2M–S2R), overexpression of Rab8a or Rab13 had no rescuing effect on the defect of neuronal polarity caused by Lgl1 depletion (Figures S2S–S2U). These results support the notion that Lgl1 acts as an upstream activator of Rab10 in regulating axon development.

Lgl1 Activates Rab10 by Releasing GDI

Interestingly, co-IP experiments showed that Myc-Lgl1 expressed in HEK293 cells preferentially interacted with Rab10^{T23N}, the GDP-locked inactive form of Rab10, rather than with the WT or the GTP-locked active form (Rab10^{Q68L}) (Figure 3A). This Lgl1 interaction with Rab10 is direct, because beads coupled with glutathione S-transferase (GST)-Rab10 fusion protein could pull down affinity-purified hexahistidine (His6)-tagged Lgl1 (Figure 3B). In line with the notion that Lgl1 preferentially interacted with GDP-locked form of Rab10, Rab10 preloaded with GDP was more effective in pulling down Lgl1 than Rab10 preloaded with GTP (Figure 3B). Thus, Lgl1 interacts directly with Rab10, preferentially in its GDP-bound form. Membrane attachment promotes Rab activation (Grosshans et al., 2006; Pfeffer, 2005; Seabra and Wasmeier, 2004). Interestingly, we found that overexpression of Lgl1 in cultured cortical neurons increased the level of membrane-associated Rab10, whereas downregulating Lgl1 with siLgl had an opposite effect (Figure 3C), in line with the observation that downregulation of Lgl1 caused diffused distribution of Rab10 (Figure S2G). However, manipulation of Lgl1 levels had no effect on the level of membrane-associated Rab8 or Cadherin (Figure 3C). Thus, Lgl1 promotes membrane association of Rab10.

The membrane attachment/detachment cycles of Rab GTPases are regulated by dissociation or association with GDI (Grosshans et al., 2006). Given that Lgl1 promotes membrane attachment of Rab10 (Figure 3C) and up- and downstream relationship of Lgl1 and Rab10, we tested the possibility that this Lgl1 effect on Rab10 may be due to Lgl1-induced dissociation of Rab10 and GDI. As shown in Figure 3D, transfected HA-Rab10 and GFP-GDI formed a complex in HEK293 cells, and this association was decreased by overexpressing Myc-Lgl1. The possibility that other molecules in HEK293 cells may be involved in this dissociation was excluded by the further experiment using cell-free systems. Beads loaded with GST-GDI, but not GST alone, could pull down HA-Rab10 expressed in HEK293 cells (Figure 3E, lanes 1 and 2). Moreover, the amount of GDI-associated Rab10 was progressively reduced by adding increasing amounts of His6-Lgl1 (Figure 3E, lanes 3–7). As a control, we showed that addition of Myosin V (aa 1320–1346), which is known to interact with Rab10 (Roland et al., 2009), had no effect on GDI-Rab10 association (Figure 3F). Furthermore, we found that Lgl1 was unable to dissociate the complex formed between GDI and Rab8a, Rab8b or Rab13 (Figure S3A), all of which have lower affinity for GDI than Rab10 (Figure S3B). Taken together, these results strongly support the notion that Lgl1 acts to release GDI from Rab10.

The dissociation of GDI from Rab10 facilitated by Lgl1 may enhance the exchange GDP for GTP (Pfeffer, 2005; Segev, 2001; Sivars et al., 2003) (see Figure 3G). This was further demonstrated in vitro by the GTP incorporation assay. For this purpose, we first expressed and purified His6-Lgl1 and GST-GDI from *E. coli*, and His6-Rab10 from Tn5 insect cells, in which Rab10 is properly prenylated (Figures S3C–S3E) and able to form a complex with GDI. We then preloaded Rab10 with GDP

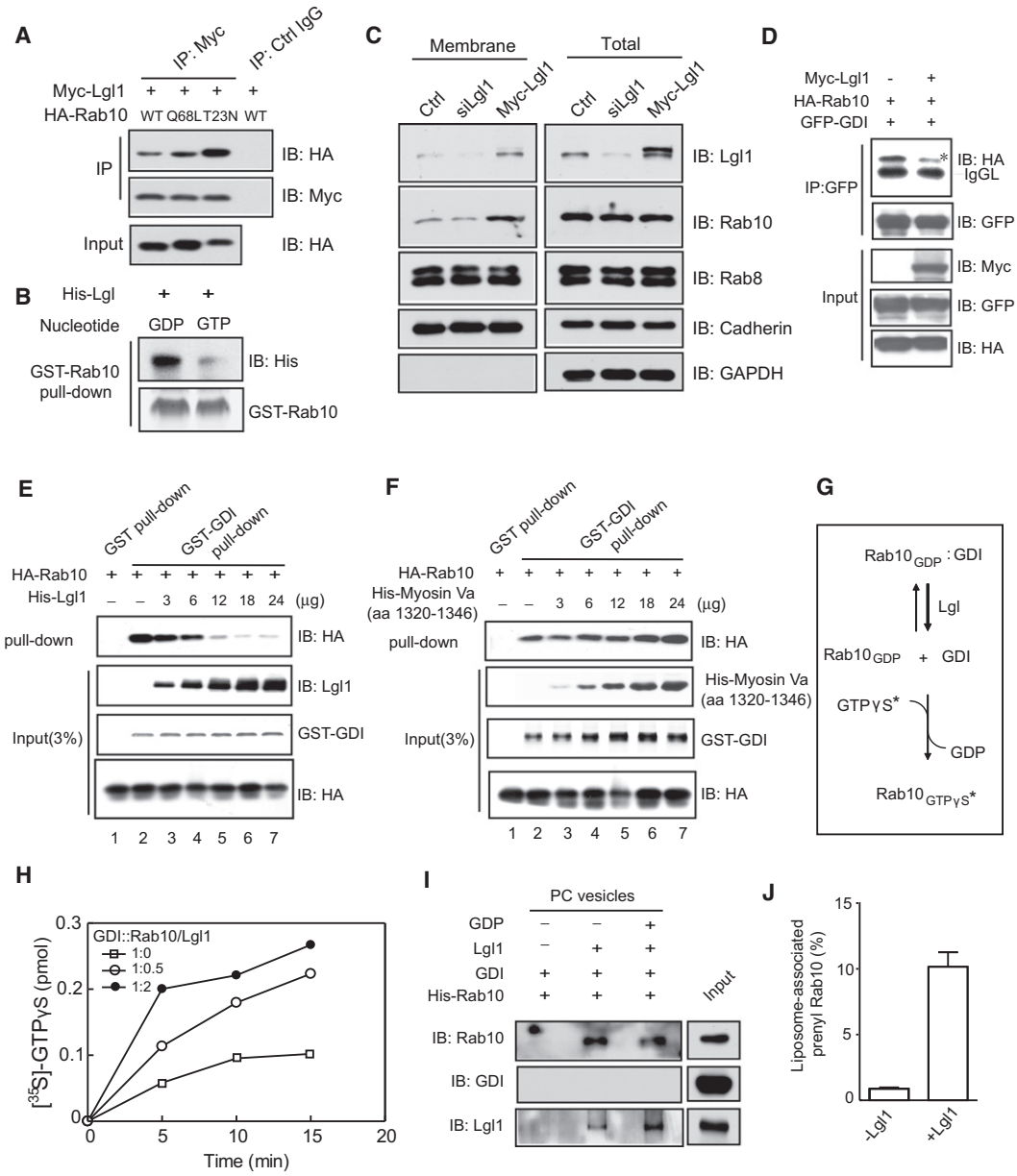

Figure 3. Lgl1 Dissociates the Rab10-GDI Complex

(A) Cell lysates from HEK293 cells transfected with indicated constructs were subject to IP and IB with indicated antibodies.

(B) GST-Rab10 immobilized on glutathione Sepharose beads were preloaded with GTP or GDP, and then incubated with purified His6-Lgl1. Bound proteins were subject to IB with indicated antibodies.

(C) Cultured cortical neurons were transfected with vector control, Myc-Lgl1, or siLgl. Membrane or total proteins were subject to IB with indicated antibodies.

(D) Lysates of HEK293 cells transfected with indicated constructs were subject to IP and IB with indicated antibodies. Note that with the presence of Myc-Lgl1, the association between GFP-GDI and HA–Rab10 was decreased (asterisk). IgGL, IgG light chain.

(E and F) HA-Rab10 expressed in HEK293 cells was affinity purified by GST-GDI immobilized on glutathione Sepharose beads, in the absence or presence of an increasing amount of purified His6-Lgl1 (E) or His6-Myosin Va (1320–1346 aa) (F). Bound proteins were subject to IB with indicated antibodies. Coomassie stain shows the amount of proteins added.

(G) Diagram for the proposed activity of Lgl1. GDI binds tightly to Rab10 and blocks release of bound GDP. Lgl1 facilitates the dissociation of Rab10 from GDI, which has intrinsic activity to exchange bound GDP for GTPγS.

(H) Lgl1 promotes incorporation of [^{35}S]GTPγS into Rab10 complexed with GDI. The Rab10-GDI complex (10 pmol) was mixed with different amounts of Lgl1 (0, 5, or 20 pmol) before performing [^{35}S]GTPγS incorporation assay. The graph shows a representative experiment of at least three repetitions.

(I and J) Rab10-GDI complex was incubated with PC liposomes in the presence or absence of purified His6-Lgl1. Liposomes were separated from soluble proteins by sucrose-gradient centrifugation. The amount of indicated proteins in the vesicle fraction was detected by IB (I) and quantitatively analyzed (J). See also Figure S3.

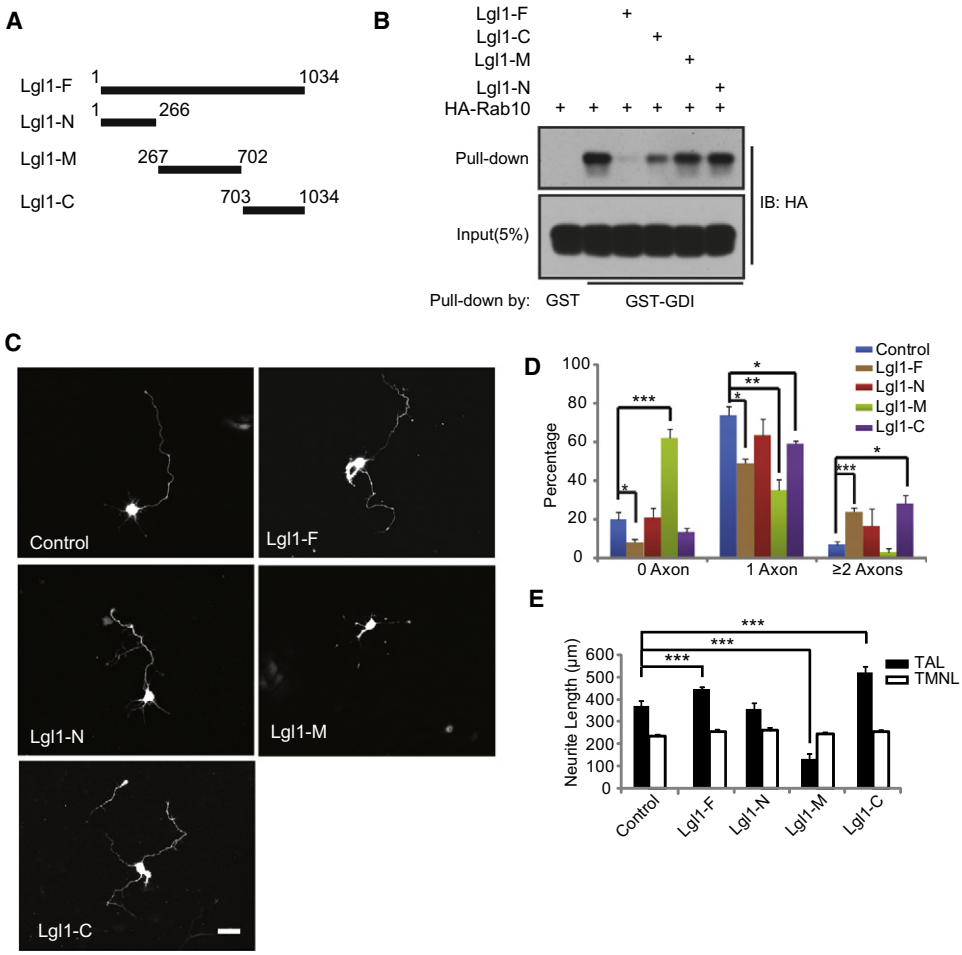

Figure 4. The GDI Displacement Activity of Lgl1 Is Involved in Axon Development

(A) Schematic representation of Lgl1 structure. Lgl1-F, full-length of Lgl1; Lgl1-N, 1–266 aa; Lgl1-M, 267–702 aa; Lgl1-C, 703–1034 aa.

(B) Lysates of HEK293 cells transfected with HA-Rab10 were incubated with beads coated with 1 μg GST-GDI. Then, the same amount (24 μg) of His6-tagged Lgl1-F or fragments (N, M, or C) was added to the bead-coupled Rab10-GDI complex, and the release of Rab10 was determined by IB.

(C) Hippocampal neurons were transfected with various Lgl1 constructs, together with GFP, and analyzed for neuronal polarity at 3 DIV. Neurons expressing GFP alone were used as control.

(D and E) Quantitative analysis for neuronal polarity (D) and neurite length (E). Results are shown as mean ± SEM of three independent experiments with at least 100 neurons. *$p < 0.05$, **$p < 0.01$, ***$p < 0.001$; ANOVA with Student's t test; scale bar represents 50 μm. See also Figure S4.

and generated Rab10-GDI complex in vitro (Figure S3F), and determined the activity of incorporating [^{35}S]GTPγS (a non-hydrolyzable GTP analog). In the absence of Lgl1, Rab10-GDI showed spontaneous [^{35}S]GTPγS incorporation that reached a plateau within 10 min (Figure 3H). Addition of purified Lgl1 elevated the uptake of [^{35}S]GTPγS by Rab10 (Figure 3H), consistent with the release of GDI from Rab10. This effect of Lgl1 was dose dependent (Figure 3H). The basal uptake of [^{35}S]GTPγS could be attributed to the intrinsic GDP/GTP exchange activity of Rab10. Finally, we tested the role of Lgl1 in promoting membrane association of Rab10 by using vesicle floating assay, which measures the effect of Lgl1 in recruiting Rab10 from the GDI-Rab10 complex into phosphatidylcholine (PC) liposomes. We found that the level of Rab10 associated with PC liposomes was undetectable in the absence of Lgl1 but markedly increased after adding Lgl1 (Figures 3I and 3J). Taken together, these results indicate that Lgl1 activates Rab10 by releasing GDI and promoting membrane association of Rab10.

GDI Displacement Activity of Lgl1 Is Involved in the Axon Development

Having determined the relation between Lgl1 and Rab10 in regulating the axon development and the role of Lgl1 as an activator for Rab10, we next determined whether the GDI displacement activity of Lgl1 is indeed involved in the axon development. For this purpose, we generated three Lgl1 fragments (aa 1–266, 267–702, or 703–1034; Figure 4A) fused with His6, and hereafter referred to as Lgl1-N, -M, or -C, respectively. We determined the effect of these Lgl1 mutants on the GDI-Rab10 complex and found that in GST-GDI pull-down experiments, the amount of GDI-associated Rab10 was reduced by adding His6-tagged full-length Lgl1 (Lgl-F) or Lgl1-C, but not Lgl1-N or -M (Figure 4B),

suggesting that the GDI displacement activity is located in the C terminus (aa 703–1034) of Lgl1. In line with this observation, Lgl1-C expressed in cultured hippocampal neurons was still associated with vesicles (Figure S4A) and localized in the membrane fraction (Figure S4B). Furthermore, Lgl1-C was sufficient to recruit Rab10 to the membrane fraction when overexpressed in cultured neurons with depletion of endogenous Lgl1 (Figure S4B). Next, we determined the effects of these truncated forms of Lgl1 on axon development. Interestingly, similar to Lgl1-F, overexpression of Lgl1-C increased the axon growth, as shown by the increased percentage of neurons with multiple axons (Figures 4C and 4D) and TAL (Figure 4E), but had no effect on TMNL (Figure 4E). In contrast, overexpression of Lgl1-M caused an opposite effect, and Lgl1-N had no effect (Figures 4C–4E). Indeed, as the substrate of aPKC, Lgl1 contains several aPKC phosphorylation sites located in the M region of Lgl1 (Betschinger et al., 2003). Overexpression of Lgl1-M may interfere with endogenous aPKC activity and thus display the dominant-negative role. Nevertheless, these results suggest that the GDI-displacement activity of Lgl1 is indeed involved in axon development.

Lgl1 and Rab10 Are Required for Directional Membrane Trafficking

To monitor membrane insertion in growing neurites, we first used BODIPY-ceramide (BODIPY FL C_5-ceramide), a fluorescent sphingomyelin and glucosylceramide precursor that exhibits concentration-dependent fluorescence—with red emission (peak at ~620 nm) when concentrated in Golgi-derived vesicles and green emission (peak at ~515 nm) after insertion and dilution in the plasmalemma (Pagano et al., 1991). As shown in Figure S5A, the pattern of signals for internalized BODIPY-ceramide was distinct from that of endosomes, which were labeled by endocytosed transferrin ligand, and displayed a Golgi-like pattern, in HEK293 cells. Next, cultured hippocampal neurons were incubated with BODIPY-ceramide for 30 min, followed by uptake for different time (0, 20, 40, or 60 min), and then washed with BSA solution to remove nonspecific surface-bound BODIPY-ceramide (see Figure S5B and Experimental Procedures). We found that BODIPY-ceramide-labeled vesicles accumulated in distal axon in time-dependent fashion, consistent with Golgi derivation (Figure S5C). The rate of BODIPY uptake was similar among different neurites of either stage 2 or stage 3 neurons (Figures S5E and S5F), when using transfected CFP to normalize the neurite volume. One hour after labeling, highest BODIPY-Red signals were observed in neurite growth cones (Figure S5C). Subsequent observation of fluorescence signals showed that the growth cone of control neurons exhibited a gradual disappearance of the red fluorescence (Figures 5A–5C), consistent with insertion of Golgi-derived vesicles into the plasma membrane. To exclude the possibility that the diminution of BODIPY-Red signals could be due to vesicle transport rather than membrane insertion, we performed live imaging to trace individual BODIPY vesicles. As shown in Figure 5A (see also Movie S1), the vesicles undergoing transportation (indicated by yellow arrowheads) exhibited little change in the intensity of BODIPY signals, whereas the signals in the growth cone remained stationary (indicated by blue and red arrowheads) and exhibited a gradual decrease in the intensity. Thus, the dissipation of BODIPY-Red signals was most likely due to membrane insertion rather than transportation. As shown by the example stage 2 neuron in a 20 hr culture in Figure 5B, we found that this dissipation was usually most rapid in the longest neurite of unpolarized neuron (Figure 5B, compare b2 with other neurites, and Figure 5D). Next, we compared membrane insertion activity between axon and dendrites of polarized neurons and found that in stage 3 neurons, membrane insertion activity was higher in axons than in dendrites (Figure 5C, compare c1 with c2 or 3, and Figure 5E). These findings are consistent with the notion that membrane addition associated with axon growth is due to insertion of Golgi-derived membrane precursors. Notably, the signal diminished along the axon in a distal to proximal direction (Figure 5C, see c1), in agreement with the observation that membrane addition happens in the distal part of the axon (Dupraz et al., 2009). Importantly, BODIPY-labeled vesicles were largely colocalized with Rab10 in axons (Figure S5D). Interestingly, in siLgl- or siRab10-transfected neurons, the reduction of the red fluorescence signal along the longest neurite of each neuron was markedly prevented, as compared to control neurons transfected with scrambled siRNA (Figure 5F). In line with the notion that Lgl1 acts through Rab10 in regulating axon development, overexpression of Rab10 prevented the membrane insertion defect in neurons with Lgl1 downregulation (Figure 5F). The general uptake of BODIPY-ceramide was unaffected by manipulating levels of Lgl1 or Rab10 (Figure S5G). These results suggest that Lgl1 and Rab10 regulate membrane insertion in growing neurites, consistent with their effects on axon development.

Lgl1 Is Associated with Plasmalemmal Precursor Vesicles and Necessary for Axonal Membrane Insertion

To further determine whether Lgl1 is indeed associated with membrane precursor vesicles, paramagnetic beads were coated with purified Lgl1 and incubated with postnuclear supernatant (PNS) from cortical neurons at 2 DIV, and the association of vesicles with beads was analyzed by transmission electron microscopy. As shown in Figure 6A, the size (~200 nm in diameter) of vesicles associated with Lgl1-coated beads is similar to that of PPVs (Pfenninger, 2009). Significantly, more vesicles were found to be associated with Lgl1-coated beads, compared to control beads coated with BSA (Figure 6B). Next, we determined the protein composition of vesicles by western blot analysis. We found that Rab10 and Rab8 were associated with Lgl1-coated beads, but not control beads, whereas Rab5 or 11 was undetectable, indicating that Lgl1-associated vesicles may be distinct from early endosomes or recycling endosomes (Figure 6C). Of note, IGFR-β, the receptor for insulin-like growth factor that has been shown to be a PPV marker (Pfenninger et al., 2003), but not synaptic vesicle protein VAMP2, was found in Lgl1-coated beads. The presence of TGN38 and absence of Bip suggested Golgi derivation of the Lgl1-associated vesicles. Interestingly, TrkB, the receptor for BDNF, and Frizzled 7, the receptor for Wnt5a, but not another axonal membrane protein L1/NgCAM (neuron-glia cell adhesion molecule) (Burack et al., 2000), were also present in Lgl1-coated beads. Indeed, both BDNF and Wnt5a have been shown to promote neuronal polarization (Shelly et al., 2007; Zhang et al., 2007). Some neuronal polarity-related proteins, including Par3, Par6, aPKC, and Dvl1,

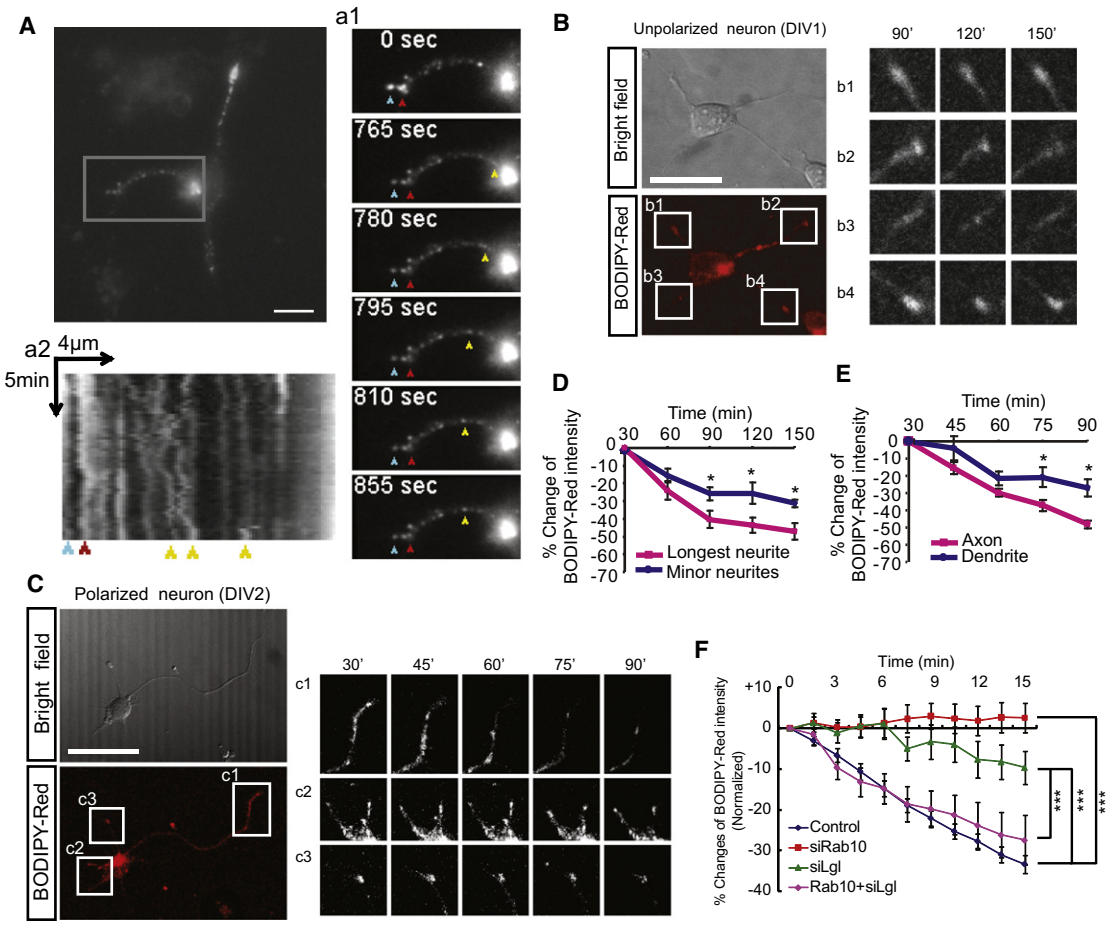

Figure 5. Lgl1 and Rab10 Affect the Polarized Membrane Trafficking in Developing Neurons

(A–C) Time-lapse images showing the changes of BODIPY-ceramide labeled vesicles in an unpolarized neuron at 1 DIV (A and B) and a polarized neuron at 2 DIV (C). Note the diminution of BODIPY-Red signals in the tip of neurite (see a1 and kymograph in a2, indicated by blue and red arrowheads). Magnified areas (B and C) show the tips of the longest neurite (b2) and other minor neurites (b1, b3, b4), or axon (c1) and dendrites (c2, c3). Scale bars, 10 μm (A), 20 μm (B), and 50 μm (C).

(D) Comparison of BODIPY-Red dissipation rate on the longest neurite and other minor neurites for unpolarized neurons at 1 DIV. Neurite volume was normalized by BODIPY-Green signals that show little change during the period of observation. *$p < 0.05$, paired t test ($n = 20$).

(E) Comparison of BODIPY-Red dissipation rate on axon and dendrites for polarized neurons at 2 DIV using BODIPY-Green to normalize neurite volume. *$p < 0.05$, paired t test ($n = 10$).

(F) Changes of BODIPY-Red signals in the longest neurites of neurons transfected with siRab10, siLgl, or siLgl plus Rab10. CFP signals expressed by pSUPER were used to normalize neurite volume. Results are shown as mean ± SEM from at least 13 neurons for each group (***$p < 0.001$, ANOVA with Student's t test). See also Figure S5 and Movie S1.

were also observed in the Lgl1 beads (Figure 6C). These results suggest a possibility that Lgl1-mediated membrane insertion may result in an increase in the local concentration and activation of signaling molecules for neuronal polarization.

Next, we directly measured membrane fusion by the observation using total internal reflection fluorescence (TIRF) microscope, which allows selective imaging of fluorescent signals located in close proximity (<200 nm) to the coverslips. First, we used Frizzled7 fused at its C terminus to GFP as a membrane marker. Cultured hippocampal neurons were cotransfected with Frizzled7-GFP and pSUPER-RFP, which encodes siRNA against Lgl1, Rab10, or scrambled sequences, and analyzed for epifluorescence or TIRF signals. As shown in Figure S6A, although epifluorescence signals of Frizzled7-GFP were detectable in all the neurites of a stage 3 neuron, the TIRF signals were present mainly in the soma and distal region of axon and the growth cone (see enlarged boxed region). This result suggests directional membrane insertion during axon development. The polarized membrane fusion was also determined using GFP-TrkB as the probe. We found that the TIRF signals of TrkB were mainly present in distal one-third of the axon and growth cone (Figure 6D), whereas the TIRF signals of transferrin receptor (TfR), a dendritic membrane protein (Burack et al., 2000), were detected mainly in soma-dendritic regions (Figure S6D). Next, we determined the role of Lgl1 and Rab10 in regulating membrane localization of Frizzled7 or TrkB. We found that in neurons transfected with siLgl1 or siRab10, although epifluorescence signals of GFP-tagged Frizzled7 or TrkB remained in the soma and neuronal tips, the TIRF signals were largely abolished (Figures 6D and 6E; Figures S6A and S6B), even in the soma.

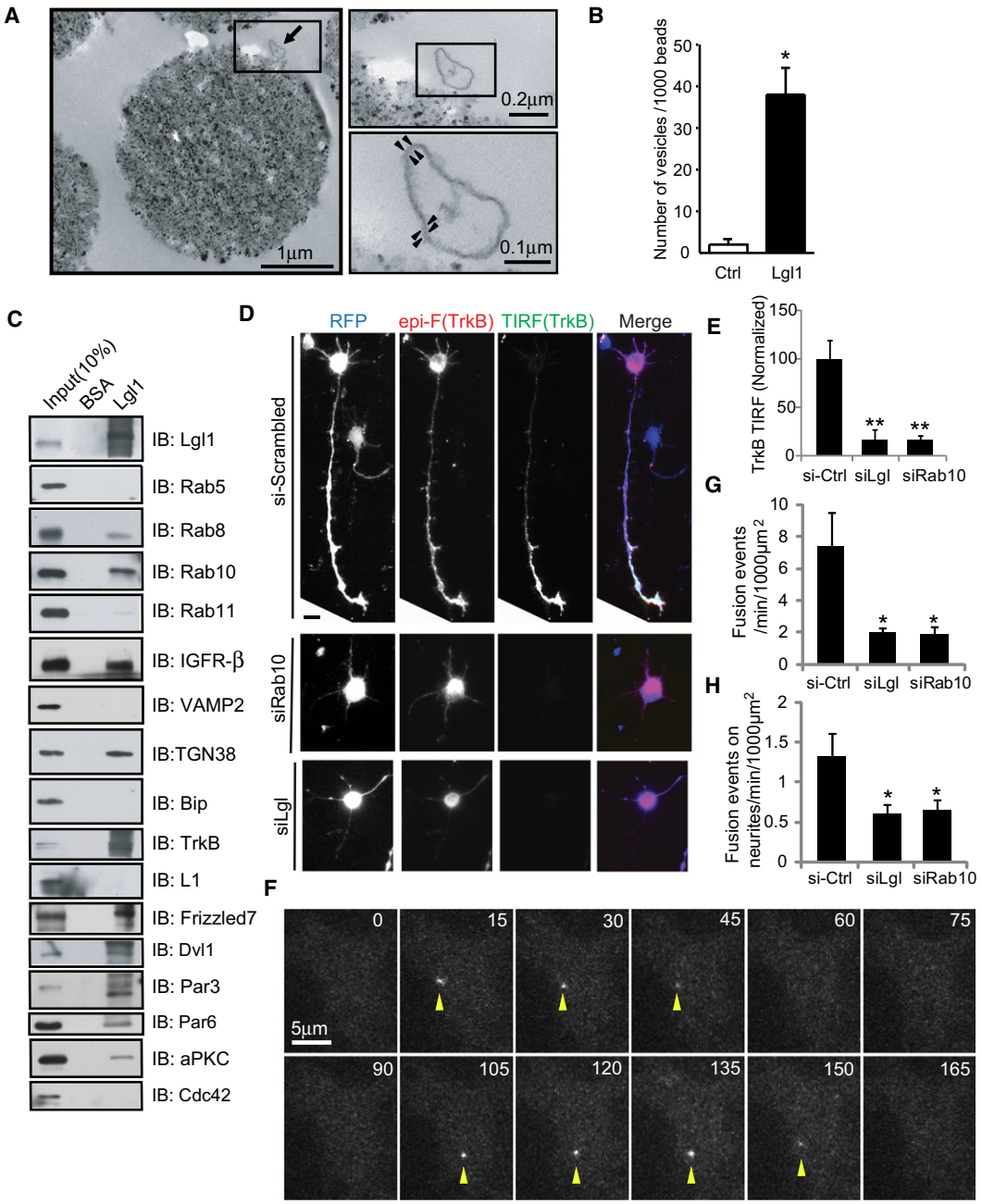

Figure 6. Lgl1 Is Associated with PPVs and Required for Directional Membrane Insertion

(A) Images by transmission electronic microscopy (TEM) showing vesicles associated with Lgl1-coated paramagnetic beads. Insets indicate an example vesicle (arrow) associated with Lgl-coated bead. Arrowheads indicate bilayer membrane of the vesicle.

(B) Number of vesicles coupled to Lgl1- or BSA-coated beads analyzed by TEM from three independent experiments. *$p < 0.05$, Student's t test.

(C) Lgl1-coated beads were subject to IB with indicated antibodies.

(D) Hippocampal neurons were cotransfected with GFP-TrkB and pSUPER-RFP vectors encoding siRNA against Lgl1, Rab10, or scrambled sequences. Epifluorescence (epi-F) and TIRF signals represent total and plasma membrane-associated TrkB, respectively.

(E) Quantification for the TIRF signals relative to epi-F signals. Average values from control group were normalized as 100. Data are presented as mean ± SEM (n = 5 neurons for each experimental group). **$p < 0.01$, Student's t test.

(F) Hippocampal neurons were transfected with TrkB-pHluorin and observed using TIRF microscope at 2 DIV. Representative images from a time-lapse display two vesicle fusion events (arrowheads).

(G and H) The frequency of vesicle fusion in the whole cell (G), including soma and neurites, and neurites (H) was quantified, respectively (n ≥ 6 cells in each group). *$p < 0.05$, Student's t test. See also Figure S6.

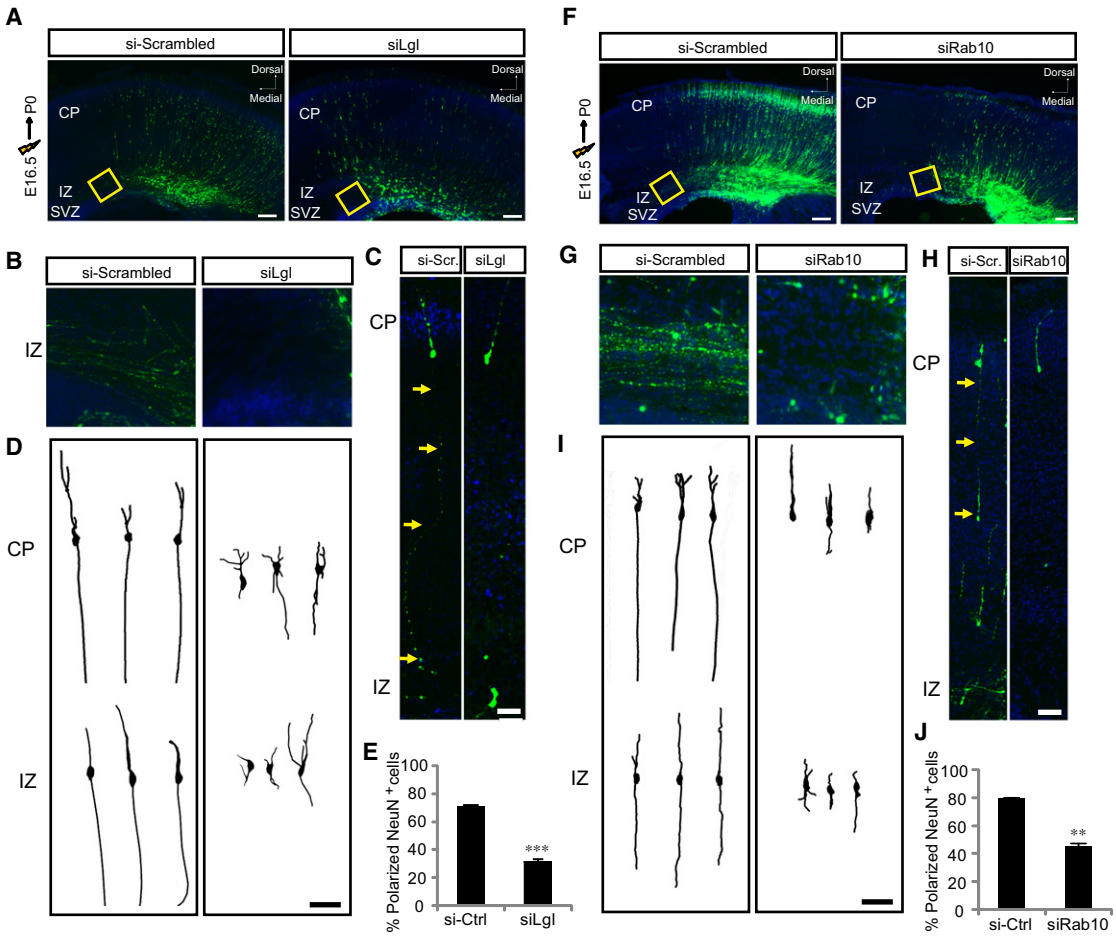

Figure 7. Lgl1 and Rab10 Are Required for Neocortical Development In Vivo

(A, B, F, and G) P0 neocortical slice from rat embryos electroporated at E16.5 with plasmids encoding siLgl (A and B), siRab10 (F and G), or respective scrambled sequences, together with YFP to label newborn neurons. Enlarged areas (B and G) indicate axons coursing through the IZ.

(C and H) Example neurons in the CP. Arrows indicate the long thin trailing axon pointing toward deep layers.

(D and I) Neurolucida traces of individual neurons in either CP or IZ regions of P0 rats.

(E and J) Quantification for polarized NeuN$^+$ cells in the CP and IZ regions. Data are presented as mean ± SEM (n = 36 for the control of siLgl, n = 40 for siLgl, n = 51 for the control of siRab10, n = 43 for siRab10). ***$p < 0.001$, **$p < 0.01$, Student's t test. Scale bars represent 200 μm in (A) and (F), and 50 μm in (C), (D), (H), and (I). See also Figure S7.

Similarly, transfection with siRab8a also decreased TIRF signals of TrkB, whereas siRab13 had no effect (Figure S6C). In support of the TIRF results, the surface staining of TrkB was abolished by downregulating Lgl1 or Rab10 (Figure S6E). In line with the finding that VAMP2 was not present in Lgl1-coated beads (Figure 6C), downregulation of Lgl1 or Rab10 had no effect on surface localization of VAMP2 (Figure S6F). Further, the role of Lgl1 and Rab10 in membrane fusion was measured in stage 1 neurons using TIRF analysis for TrkB tagged with pHluorin (Miesenböck et al., 1998), which has low fluorescence intensity when remaining within the acidic vesicle lumen and exhibits a fast increase in fluorescence signals when exposed to higher pH upon fusion with plasma membrane (see Figure 6F for fusion events). The fusion events in the soma and neurites were quantified, respectively. As shown in Figure 6G and 6H, downregulation of Lgl1 or Rab10 caused a remarkable decrease in the membrane fusion in either the whole cell or neurites. Thus, Lgl1 and Rab10 are required for directional membrane fusion during axon development.

Lgl1 and Rab10 Are Needed for Neuronal Polarization In Vivo

To determine the effects of Lgl1 or Rab10 in the differentiation of newborn neurons, E16.5 rat embryos were subject to in utero electroporation with plasmids encoding siLgl, siRab10, or respective scrambled sequences, together with pCAG-IRES-EYFP to label cortical neural precursors. Four days after electroporation, the development of YFP-positive cells was examined at P0 (Figures 7A and 7F). First, neuronal fate was determined by staining with antibodies against NeuN, a marker for mature neurons, or Ki67, which labels proliferating cells. We found that siLgl transfection caused an increase in the percentage of Ki67-positive (Ki67$^+$) cells and a decrease in the percentage of NeuN-positive (NeuN$^+$) cells (Figures S7A–S7D), in agreement

with a previous observation that Lgl1 affects differentiation of neuronal precursors in the VZ (Klezovitch et al., 2004). Whereas bundles of axons traversing through the intermediate zone (IZ) were observed in control animals, such axonal projection was not seen in siLgl-transfected animals (Figures 7A and 7B). Such defects could be caused by abnormal neuronal fate determination or morphogenesis. To circumvent the multifaceted role of Lgl1, we analyzed morphology of $NeuN^+$ neurons located in the IZ and CP regions. Interestingly, whereas most neurons of control animals exhibited polarized structures with a leading process destined to become dendrite and a long trailing process destined to become axon, in the CP or IZ regions, a number of neurons in animals transfected with siLgl failed to polarize normally (Figures 7C–7E). Thus, Lgl1 is needed for neuronal polarization in vivo.

The same approach was used to determine the role of Rab10 in the differentiation of cortical neurons. Unlike that of Lgl1, Rab10 had no effect on neuronal fate determination because transfection with siRab10 had no effect on the percentage of $NeuN^+$ or $Ki67^+$ cells (Figures S7E–S7H). Nevertheless, severe defects in axon development were observed in neurons with Rab10 downregulation (Figures 7F–7J), as reflected from the loss of axonal bundles coursing through the IZ (Figures 7F and 7G) and failure of CP or IZ neurons to extend the long trailing axon (Figures 7H and 7I). Indeed, 79.3% ± 0.9% of control neurons possessed a morphologically polarized structure compared to 45% ± 2.7% of siRab10-transfected neurons (Figure 7J). In addition to the defects in axon formation, downregulation of Lgl1 or Rab10 also impaired migration of newborn neurons to the CP. As shown in Figures 7A and 7F, whereas a large population of control cells was found in the CP on P0, lesser siLgl- or siRab10-transfected neurons were observed in the CP. Given the polarity defects of $NeuN^+$ neurons in the CP and IZ of animals with downregulation of Lgl1 or Rab10, we conclude that the Lgl1/Rab10 system is required for axon specification both in vivo and in vitro. We also determined the role of Rab8a and Rab13 and found that downregulation of both Rabs appeared to affect neuronal migration (Figure S7I), and, consistent with the results obtained in cultured neurons, downregulation of Rab8a, but not Rab13, impaired axon development in vivo (Figures S7J–S7M). The regulatory or functioning mechanisms for Rab8 need further investigation.

DISCUSSION

Studies of the molecular mechanisms underlying axon development have identified a number of key molecules involved in triggering axon specification and growth (Arimura and Kaibuchi, 2007; Barnes and Polleux, 2009). Many of these molecules are believed to exert their action by regulating cytoskeleton organization (Barnes et al., 2007; Bradke and Dotti, 1999; Chen et al., 2006; Jiang et al., 2005; Kishi et al., 2005; Schwamborn and Püschel, 2004; Shelly et al., 2007; Witte et al., 2008; Yoshimura et al., 2005). Another important cellular process critical for axon development is the directed membrane trafficking underlying the insertion of new membrane associated with axon growth, an aspect of axon development that remains poorly understood. In this study, we show that Lgl1 plays an important role in directional membrane insertion underlying axon development, by activating Rab10.

Cultured hippocampal neurons can undergo spontaneous polarization, with one thin axon and multiple dendrites. In this system, specification of axon-dendrite polarity is preceded by the accelerated growth of only one neurite, which depends on asymmetric insertion of new plasma membrane mediated by directional vesicle recruitment and exocytic fusion (Dupraz et al., 2009; Futerman and Banker, 1996; Pfenninger, 2009). The role of the Lgl1-Rab10 system in directing membrane trafficking was investigated here by using BODIPY-ceramide to label PPVs or analyzing the TIRF signals of TrkB or Frizzled7 in the growing neurites. We propose that membrane-associated Lgl1 recruits Rab10 to the membrane by dissociating Rab10 from GDI, and activation of membrane-bound Rab10 may trigger multiple steps required for addition of new membrane, including vesicle recruitment and sorting, as well as vesicle docking and fusion at the plasma membrane. In line with the finding that the Lgl1-Rab10 system regulates vesicle trafficking, we found that both Lgl1 and Rab10 are required for axon development in cultured hippocampal neurons, as shown by axon differentiation and elongation, and neocortical neuronal polarization in vivo. That Lgl1 is a positive regulator of Rab10 is also supported by the finding that Lgl1 acts upstream of Rab10 in promoting axon development (Figures 2J–2M). How might Lgl1 itself be regulated during neuronal polarization? A recent report showed that the mammalian homologs of yeast exocyst complex influence neuronal polarity through aPKC (Lalli, 2009), which is known to regulate Lgl homologs in other systems. Furthermore, Lgl1 has been shown to be regulated by Dvl (Dollar et al., 2005). It is thus possible that Dvl/aPKC may act as upstream regulators of the Lgl1-Rab10 system. It has been shown that vesicle-SNARE (soluble *N*-ethylmaleimide-sensitive fusion protein attachment protein receptor) proteins, such as VAMP2, VAMP4, or VAMP7, are involved in the exocytic machinery that drives neuritogenesis (Cocucci et al., 2008; Gupton and Gertler, 2010; Martinez-Arca et al., 2000). However, we found that VAMP2 was not associated with Lgl1-coated beads (Figure 6C), and downregulation of Lgl1 or Rab10 had no effect on membrane localization of VAMP2 (Figure S6F). Nevertheless, these results cannot exclude the possible interaction between the Lgl1-Rab10 system and other SNARE proteins.

Among more than 60 mammalian Rab proteins, several have been shown to regulate neuronal development and membrane trafficking, besides Rab10 shown here. For example, Rab27 activation promotes retrograde trafficking of BDNF/TrkB endosomes (Arimura et al., 2009), and Rab3 activation promotes membrane fusion of presynaptic vesicles (Geppert et al., 1997; Schlüter et al., 2004), whereas Rab5 and Rab11 activation inhibits neurite outgrowth (Liu et al., 2007; Shirane and Nakayama, 2006). Similar to Rab10, downregulation of Rab8 affected membrane insertion as well as neuronal morphogenesis (Huber et al., 1995). More recently, several Rab proteins, including Rab5, Rab7, and Rab11, have been shown to be involved in multiple phases of neuronal migration through distinct endocytic pathways (Kawauchi et al., 2010). Different Rabs may have distinct regulatory mechanisms. For example, DENND4 family proteins have been identified as specific GEFs for Rab10, rather than Rab8 or Rab13 (Yoshimura et al., 2010).

Given the diverse roles of different Rab GTPases in mammalian cells, it is of great interest to identify new regulatory factors besides proteins in the GEF and GAP families.

Given that Rab-dependent directional membrane trafficking is crucial for a number of polarization processes, the Lgl1-Rab10 system may also function within other cellular contexts, including membrane receptor insertion, asymmetric membrane distribution of cell fate determinants, axon guidance, as well as cell migration.

EXPERIMENTAL PROCEDURES

Reagents and Biochemical Analysis

All reagents, including antibodies, siRNAs, and constructs used in this study are introduced in the Supplemental Experimental Procedures. Recombinant proteins used in this study were affinity purified from *E. coli* BL21 or Tn5 insect cells with glutathione Sepharose or Ni-NTA agarose column, respectively. Lysates or membrane fractions of transfected HEK293 cells or primary neurons were subject to immunoprecipitation or pull-down analysis. The [γ^{35}S]GTP incorporation assay was performed following the protocol described in a previous report (Sivars et al., 2003). Rab10 recruitment onto liposomes was analyzed following a previous report (Machner and Isberg, 2007). See Supplemental Experimental Procedures for details.

Vesicle-Binding Assay

Paramagnetic beads (Dynal) were coated with His6-Lgl1 according to the manufacturer's instructions. Cortical neurons at 2 DIV were homogenized with PBS containing 250 mM sucrose, 0.5 mM DTT, and protease inhibitors, followed by centrifugation at 10, 000 × g for 10 min to generate postnuclear supernatant (PNS) fraction (Machner and Isberg, 2006). The His6-Lgl1-coated beads were incubated with PNS for 4 hr at 4°C, followed by extensive washes. The pelleted beads were then processed for electron microscopy or immunoblotting analysis.

Neuron Culture, Electroporation, and Imaging

Rat hippocampal neurons were prepared as described previously (Chen et al., 2006). Dissociated neurons were transfected by electroporation using the Amaxa Nucleofector device, followed by imaging analysis for neuronal polarity, subcellular localization, or TIRF signals. In utero electroporation was performed as described previously (Saito and Nakatsuji, 2001), and all animal usage followed guidelines by the Institutional Animal Care and Use Committee of the Institute of Neuroscience, Chinese Academy of Sciences. See Supplemental Experimental Procedures for details.

BODIPY-Ceramide Labeling and Fluorescence Observation

Hippocampal neurons cultured in vitro for 12–48 hr were incubated with 5 μM BODIPY FL C_5-ceramide conjugated with BSA for 30 min in room temperature, followed by three washes with HBSS to remove free dye, and subsequent incubation at 37°C for different times (0–60 min) to induce the endocytic uptake of source-absorbed BODIPY-ceramide, and then undergo three washes (within 0.5 hr) with 5% BSA solution to remove surface-bound nonspecific BODIPY-ceramide. Fluorescence signals for live neurons were viewed and collected using individual filter set (525 ± 25 nm for green, >575 nm for red, and 482 ± 25 nm for CFP). Details for software analysis of images are presented in Supplemental Experimental Procedures.

Quantitative Analysis

To quantify neuronal polarity, neurites positive for SMI-312 and longer than 100 μm were considered as axon. The TAL or TMNL (SMI-312 negative and <100 μm in length) was measured, respectively. For those cells without axon, the value of axon length was assigned as 0 μm. After analysis for the normal distribution and homogeneity of variance among values of the same set, these data were subject to statistical analysis using one-way analysis of variance (ANOVA) supplemented with t tests. All the data are shown as mean ± SEM from at least three experiments ($p < 0.05$ is considered as significant difference).

SUPPLEMENTAL INFORMATION

Supplemental Information includes seven figures, Supplemental Experimental Procedures, and one movie and can be found with this article online at doi:10.1016/j.devcel.2011.07.007.

ACKNOWLEDGMENTS

We thank Dr. M.-M. Poo for the comments on the manuscript. We are grateful to Dr. K.H. Baek for Lgl1 construct, Dr. K.I. Nakayama for Rab4, 5, and 11 constructs, Dr. G. Banker for TfR-GFP construct, Dr. G. Miesenbock for pHluorin plasmid, Dr. J. Sanes for VAMP2-BTX-Tag plasmid, Dr. G. Wang for the help with protein expression, Dr. J.P. Ding for constructive suggestions on the Rab10-GDI complex purification, and Dr. Q. Hu of ION Imaging Facility for microscope analysis. This work was supported by National Basic Research Program (2011CB809002), Chinese Academy of Sciences Project (XDA01020305), and National Natural Science Foundation of China (31021063 and 30825013).

Received: January 24, 2011
Revised: May 10, 2011
Accepted: July 14, 2011
Published online: August 18, 2011

REFERENCES

Arimura, N., and Kaibuchi, K. (2007). Neuronal polarity: from extracellular signals to intracellular mechanisms. Nat. Rev. Neurosci. *8*, 194–205.

Arimura, N., Kimura, T., Nakamuta, S., Taya, S., Funahashi, Y., Hattori, A., Shimada, A., Ménager, C., Kawabata, S., Fujii, K., et al. (2009). Anterograde transport of TrkB in axons is mediated by direct interaction with Slp1 and Rab27. Dev. Cell *16*, 675–686.

Barnes, A.P., and Polleux, F. (2009). Establishment of axon-dendrite polarity in developing neurons. Annu. Rev. Neurosci. *32*, 347–381.

Barnes, A.P., Lilley, B.N., Pan, Y.A., Plummer, L.J., Powell, A.W., Raines, A.N., Sanes, J.R., and Polleux, F. (2007). LKB1 and SAD kinases define a pathway required for the polarization of cortical neurons. Cell *129*, 549–563.

Betschinger, J., Mechtler, K., and Knoblich, J.A. (2003). The Par complex directs asymmetric cell division by phosphorylating the cytoskeletal protein Lgl. Nature *422*, 326–330.

Bilder, D., Li, M., and Perrimon, N. (2000). Cooperative regulation of cell polarity and growth by *Drosophila* tumor suppressors. Science *289*, 113–116.

Bradke, F., and Dotti, C.G. (1999). The role of local actin instability in axon formation. Science *283*, 1931–1934.

Burack, M.A., Silverman, M.A., and Banker, G. (2000). The role of selective transport in neuronal protein sorting. Neuron *26*, 465–472.

Chen, Y.M., Wang, Q.J., Hu, H.S., Yu, P.C., Zhu, J., Drewes, G., Piwnica-Worms, H., and Luo, Z.G. (2006). Microtubule affinity-regulating kinase 2 functions downstream of the PAR-3/PAR-6/atypical PKC complex in regulating hippocampal neuronal polarity. Proc. Natl. Acad. Sci. USA *103*, 8534–8539.

Cocucci, E., Racchetti, G., Rupnik, M., and Meldolesi, J. (2008). The regulated exocytosis of enlargeosomes is mediated by a SNARE machinery that includes VAMP4. J. Cell Sci. *121*, 2983–2991.

Dollar, G.L., Weber, U., Mlodzik, M., and Sokol, S.Y. (2005). Regulation of Lethal giant larvae by Dishevelled. Nature *437*, 1376–1380.

Dotti, C.G., Sullivan, C.A., and Banker, G.A. (1988). The establishment of polarity by hippocampal neurons in culture. J. Neurosci. *8*, 1454–1468.

Dupraz, S., Grassi, D., Bernis, M.E., Sosa, L., Bisbal, M., Gastaldi, L., Jausoro, I., Cáceres, A., Pfenninger, K.H., and Quiroga, S. (2009). The TC10-Exo70 complex is essential for membrane expansion and axonal specification in developing neurons. J. Neurosci. *29*, 13292–13301.

Futerman, A.H., and Banker, G.A. (1996). The economics of neurite outgrowth—the addition of new membrane to growing axons. Trends Neurosci. *19*, 144–149.

Gateff, E. (1978). Malignant neoplasms of genetic origin in *Drosophila melanogaster*. Science *200*, 1448–1459.

Geppert, M., Goda, Y., Stevens, C.F., and Südhof, T.C. (1997). The small GTP-binding protein Rab3A regulates a late step in synaptic vesicle fusion. Nature *387*, 810–814.

Goslin, K., and Banker, G. (1989). Experimental observations on the development of polarity by hippocampal neurons in culture. J. Cell Biol. *108*, 1507–1516.

Grosshans, B.L., Andreeva, A., Gangar, A., Niessen, S., Yates, J.R., 3rd, Brennwald, P., and Novick, P. (2006). The yeast lgl family member Sro7p is an effector of the secretory Rab GTPase Sec4p. J. Cell Biol. *172*, 55–66.

Gupton, S.L., and Gertler, F.B. (2010). Integrin signaling switches the cytoskeletal and exocytic machinery that drives neuritogenesis. Dev. Cell *18*, 725–736.

Huber, L.A., Dupree, P., and Dotti, C.G. (1995). A deficiency of the small GTPase rab8 inhibits membrane traffic in developing neurons. Mol. Cell. Biol. *15*, 918–924.

Hutterer, A., Betschinger, J., Petronczki, M., and Knoblich, J.A. (2004). Sequential roles of Cdc42, Par-6, aPKC, and Lgl in the establishment of epithelial polarity during *Drosophila* embryogenesis. Dev. Cell *6*, 845–854.

Ishikura, S., and Klip, A. (2008). Muscle cells engage Rab8A and myosin Vb in insulin-dependent GLUT4 translocation. Am. J. Physiol. Cell Physiol. *295*, C1016–C1025.

Jiang, H., Guo, W., Liang, X., and Rao, Y. (2005). Both the establishment and the maintenance of neuronal polarity require active mechanisms: critical roles of GSK-3beta and its upstream regulators. Cell *120*, 123–135.

Kawauchi, T., Sekine, K., Shikanai, M., Chihama, K., Tomita, K., Kubo, K., Nakajima, K., Nabeshima, Y., and Hoshino, M. (2010). Rab GTPases-dependent endocytic pathways regulate neuronal migration and maturation through N-cadherin trafficking. Neuron *67*, 588–602.

Kishi, M., Pan, Y.A., Crump, J.G., and Sanes, J.R. (2005). Mammalian SAD kinases are required for neuronal polarization. Science *307*, 929–932.

Klezovitch, O., Fernandez, T.E., Tapscott, S.J., and Vasioukhin, V. (2004). Loss of cell polarity causes severe brain dysplasia in Lgl1 knockout mice. Genes Dev. *18*, 559–571.

Lalli, G. (2009). RalA and the exocyst complex influence neuronal polarity through PAR-3 and aPKC. J. Cell Sci. *122*, 1499–1506.

Lehman, K., Rossi, G., Adamo, J.E., and Brennwald, P. (1999). Yeast homologues of tomosyn and lethal giant larvae function in exocytosis and are associated with the plasma membrane SNARE, Sec9. J. Cell Biol. *146*, 125–140.

Liu, J., Lamb, D., Chou, M.M., Liu, Y.J., and Li, G. (2007). Nerve growth factor-mediated neurite outgrowth via regulation of Rab5. Mol. Biol. Cell *18*, 1375–1384.

Machner, M.P., and Isberg, R.R. (2006). Targeting of host Rab GTPase function by the intravacuolar pathogen Legionella pneumophila. Dev. Cell *11*, 47–56.

Machner, M.P., and Isberg, R.R. (2007). A bifunctional bacterial protein links GDI displacement to Rab1 activation. Science *318*, 974–977.

Martinez-Arca, S., Alberts, P., Zahraoui, A., Louvard, D., and Galli, T. (2000). Role of tetanus neurotoxin insensitive vesicle-associated membrane protein (Tl-VAMP) in vesicular transport mediating neurite outgrowth. J. Cell Biol. *149*, 889–900.

Miesenböck, G., De Angelis, D.A., and Rothman, J.E. (1998). Visualizing secretion and synaptic transmission with pH-sensitive green fluorescent proteins. Nature *394*, 192–195.

Ohshiro, T., Yagami, T., Zhang, C., and Matsuzaki, F. (2000). Role of cortical tumour-suppressor proteins in asymmetric division of *Drosophila* neuroblast. Nature *408*, 593–596.

Pagano, R.E., Martin, O.C., Kang, H.C., and Haugland, R.P. (1991). A novel fluorescent ceramide analogue for studying membrane traffic in animal cells: accumulation at the Golgi apparatus results in altered spectral properties of the sphingolipid precursor. J. Cell Biol. *113*, 1267–1279.

Peng, C.Y., Manning, L., Albertson, R., and Doe, C.Q. (2000). The tumour-suppressor genes lgl and dlg regulate basal protein targeting in *Drosophila* neuroblasts. Nature *408*, 596–600.

Pfeffer, S.R. (2001). Rab GTPases: specifying and deciphering organelle identity and function. Trends Cell Biol. *11*, 487–491.

Pfeffer, S. (2005). A model for Rab GTPase localization. Biochem. Soc. Trans. *33*, 627–630.

Pfenninger, K.H. (2009). Plasma membrane expansion: a neuron's Herculean task. Nat. Rev. Neurosci. *10*, 251–261.

Pfenninger, K.H., Laurino, L., Peretti, D., Wang, X., Rosso, S., Morfini, G., Cáceres, A., and Quiroga, S. (2003). Regulation of membrane expansion at the nerve growth cone. J. Cell Sci. *116*, 1209–1217.

Plant, P.J., Fawcett, J.P., Lin, D.C., Holdorf, A.D., Binns, K., Kulkarni, S., and Pawson, T. (2003). A polarity complex of mPar-6 and atypical PKC binds, phosphorylates and regulates mammalian Lgl. Nat. Cell Biol. *5*, 301–308.

Roland, J.T., Lapierre, L.A., and Goldenring, J.R. (2009). Alternative splicing in class V myosins determines association with Rab10. J. Biol. Chem. *284*, 1213–1223.

Saito, T., and Nakatsuji, N. (2001). Efficient gene transfer into the embryonic mouse brain using in vivo electroporation. Dev. Biol. *240*, 237–246.

Sano, H., Eguez, L., Teruel, M.N., Fukuda, M., Chuang, T.D., Chavez, J.A., Lienhard, G.E., and McGraw, T.E. (2007). Rab10, a target of the AS160 Rab GAP, is required for insulin-stimulated translocation of GLUT4 to the adipocyte plasma membrane. Cell Metab. *5*, 293–303.

Schlüter, O.M., Schmitz, F., Jahn, R., Rosenmund, C., and Südhof, T.C. (2004). A complete genetic analysis of neuronal Rab3 function. J. Neurosci. *24*, 6629–6637.

Schwamborn, J.C., and Püschel, A.W. (2004). The sequential activity of the GTPases Rap1B and Cdc42 determines neuronal polarity. Nat. Neurosci. *7*, 923–929.

Seabra, M.C., and Wasmeier, C. (2004). Controlling the location and activation of Rab GTPases. Curr. Opin. Cell Biol. *16*, 451–457.

Segev, N. (2001). Ypt and Rab GTPases: insight into functions through novel interactions. Curr. Opin. Cell Biol. *13*, 500–511.

Shelly, M., Cancedda, L., Heilshorn, S., Sumbre, G., and Poo, M.M. (2007). LKB1/STRAD promotes axon initiation during neuronal polarization. Cell *129*, 565–577.

Shi, S.H., Jan, L.Y., and Jan, Y.N. (2003). Hippocampal neuronal polarity specified by spatially localized mPar3/mPar6 and PI 3-kinase activity. Cell *112*, 63–75.

Shirane, M., and Nakayama, K.I. (2006). Protrudin induces neurite formation by directional membrane trafficking. Science *314*, 818–821.

Sivars, U., Aivazian, D., and Pfeffer, S.R. (2003). Yip3 catalyses the dissociation of endosomal Rab-GDI complexes. Nature *425*, 856–859.

Stenmark, H. (2009). Rab GTPases as coordinators of vesicle traffic. Nat. Rev. Mol. Cell Biol. *10*, 513–525.

Sun, Y., Bilan, P.J., Liu, Z., and Klip, A. (2010). Rab8A and Rab13 are activated by insulin and regulate GLUT4 translocation in muscle cells. Proc. Natl. Acad. Sci. USA *107*, 19909–19914.

Wirtz-Peitz, F., and Knoblich, J.A. (2006). Lethal giant larvae take on a life of their own. Trends Cell Biol. *16*, 234–241.

Witte, H., Neukirchen, D., and Bradke, F. (2008). Microtubule stabilization specifies initial neuronal polarization. J. Cell Biol. *180*, 619–632.

Ye, B., Zhang, Y.W., Jan, L.Y., and Jan, Y.N. (2006). The secretory pathway and neuron polarization. J. Neurosci. *26*, 10631–10632.

Yoshimura, T., Kawano, Y., Arimura, N., Kawabata, S., Kikuchi, A., and Kaibuchi, K. (2005). GSK-3beta regulates phosphorylation of CRMP-2 and neuronal polarity. Cell *120*, 137–149.

Yoshimura, S., Gerondopoulos, A., Linford, A., Rigden, D.J., and Barr, F.A. (2010). Family-wide characterization of the DENN domain Rab GDP-GTP exchange factors. J. Cell Biol. *191*, 367–381.

Zhang, X., Wang, P., Gangar, A., Zhang, J., Brennwald, P., TerBush, D., and Guo, W. (2005). Lethal giant larvae proteins interact with the exocyst complex and are involved in polarized exocytosis. J. Cell Biol. *170*, 273–283.

Zhang, X., Zhu, J., Yang, G.Y., Wang, Q.J., Qian, L., Chen, Y.M., Chen, F., Tao, Y., Hu, H.S., Wang, T., and Luo, Z.G. (2007). Dishevelled promotes axon differentiation by regulating atypical protein kinase C. Nat. Cell Biol. *9*, 743–754.